Assessment of a portable UV–Vis spectrophotometer's performance for stream water DOC and Fe content monitoring in remote areas

Zhu, Xudan; Chen, Liang; Pumpanen, Jukka; Keinänen, Markku; Laudon, Hjalmar ...

2021-03-01
Elsevier B.V.
http://hdl.handle.net/10138/351355
Zhu, X, Chen, L, Pumpanen, J, Keinänen, M, Laudon, H, Ojala, A, Palviainen, M, Kiirikki, M, Neitola, K & Berninger, F 2021, 'Assessment of a portable UV–Vis spectrophotometer's performance for stream water DOC and Fe content monitoring in remote areas', Talanta, vol. 224, 121919. https://doi.org/10.1016/j.talanta.2020.121919

Assessment of a portable UV–Vis spectrophotometer's performance for stream water DOC and Fe content monitoring in remote areas

Xudan Zhu [a,*], Liang Chen [a], Jukka Pumpanen [b], Markku Keinänen [a], Hjalmar Laudon [c], Anne Ojala [d, e, f], Marjo Palviainen [g], Mikko Kiirikki [h], Kimmo Neitola [i], Frank Berninger [a]

[a] *Department of Environmental and Biological Sciences University of Eastern Finland, 80101 Joensuu, Finland*

[b] *Department of Environmental and Biological Sciences, University of Eastern Finland, 70211 Kuopio, Finland*

[c] *Department of Forest Ecology and Management, Swedish University of Agricultural Sciences, 90183 Umeå, Sweden*

[d] *Faculty of Biological and Environmental Sciences, Ecosystems and Environment Research Programme, University of Helsinki, Lahti, Finland*

[e] *Institute for Atmospheric and Earth System Research/Forest Sciences, Faculty of Agriculture and Forestry, University of Helsinki, 00014 Helsinki, Finland*

[f] *Faculty of Biological and Environmental Sciences, Helsinki Institute of Sustainability Science, University of Helsinki, 00014 Helsinki, Finland*

[g] *Department of Forest Science, University of Helsinki, 00014 Helsinki, Finland*

[h] *Luode Consulting Sinimäentie 10 B, 02630 Espoo, Finland*

[i] *Institute for Atmospheric and Earth System Research (INAR), University of Helsinki, 00014 Helsinki, Finland.*

Corresponding Author: Xudan Zhu

Email Adress: xudanzhu@uef.fi

Institution: University of Estern Finland, *80101 Joensuu, Finland*

Postal Address: Natura building 375a, Yliopistokatu 2, FI-80100 Joensuu, Finland

Phone Number: +358403617280

Abstract

Quantification of dissolved organic carbon (DOC) and iron (Fe) in surface waters is critical for understanding the water quality dynamics, brownification and carbon balance in the northern hemisphere. Especially in the remote areas, sampling and laboratory analysis of DOC and Fe content at a sufficient temporal frequency is difficult. Ultraviolet-visible (UV-Vis) spectrophotometry is a promising tool for water quality monitoring to increase the sampling frequency and applications in remote regions. The aim of this study was (1) to investigate the performance of an in-situ UV-Vis spectrophotometer for detecting spectral absorbances in comparison with a laboratory benchtop instrument; (2) to analyse the stability of DOC and Fe estimates from UV-Vis spectrophotometers among different rivers using multivariate methods; (3) to compare site-specific calibration of models

to pooled models and investigate the extrapolation of DOC and Fe predictions from one catchment to another. This study indicates that absorbances that were measured by UV-Vis sensor explained 96% of the absorbance data from the laboratory benchtop instrument. Among the three tested multivariate methods, multiple stepwise regression (MSR) was the best model for both DOC and Fe predictions. Accurate and unbiased models for multiple watersheds for DOC were built successfully, and these models could be extrapolated from one watershed to another even without site-specific calibration for DOC. However, for Fe the combination of different datasets was not possible.

Key Words:

Water quality, UV-Vis spectrophotometer, Spectral absorbance, Dissolved organic matter, Ferric iron

1. Introduction

Globally inland waters are a sink for 600 million tn C y^{-1} and deliver an additional ~900 million to 1 200 million tn C y^{-1} to the oceans of which a majority is in organic forms (Aufdenkampe et al., 2011; Cole et al., 2007). With estimates of the global land sink to be around 2 400 million tn C y^{-1} (Mercado et al., 2009), the C exports via inland waters would account for about half of the net terrestrial C sink. It has been frequently reported that water colour is becoming darker in many lakes and running waters of the Northern hemisphere (Asmala et al., 2019; Erlandsson et al., 2011; Haaland et al., 2010; Peltomaa et al., 2014). The drivers behind this trend, sometimes referred to as brownification, are heavily debated and have been ascribed to hydrological factors (Erlandsson et al., 2008; Hongve et al., 2004) as well as an increase in temperature, changes in land-use and reduced acid deposition (Asmala et al., 2019). Although it is difficult to tease out any single factor causing brownification, brownification is directly due to the increased dissolved organic matter (DOM) and iron (Fe) concentrations (Haaland et al., 2010; Maloney et al., 2005). Much of the export of DOC and

Fe occurs during extreme rainfall or snowmelt events (Raymond et al., 2016), which makes the high frequency monitoring of pulse events necessary. However, pulse events are usually of short duration and challenging to capture using physical water sampling.

The development of continuously operating water quality sensors has led to a transition from studying long-term trends and seasonal patterns to the investigation of highly dynamic phenomena, such as storm events and diurnal patterns, using high-frequency in situ measurements (Jacobs et al. 2020). With the currently available technology and decreasing costs, in situ sensors are more frequently used for monitoring, especially in remote areas (Langergraber et al. 2003; Avagyan et al. 2014; Rode et al. 2016). Although large amounts of data present challenges regarding storage, processing, and analysis (McDowell, 2015), long-term monitoring datasets provide an opportunity for detailed investigations of hydrological and biogeochemical processes in dynamic systems (Kirchner et al. 2004; Krause et al. 2015; Rode et al. 2016).

UV-Vis sensors are an emerging technology to measure and monitor concentrations of dissolved organic carbon (DOC) in situ. These commercially available sensors are spectrophotometers in the UV-visible spectrum. They can be used for in situ real-time measurements at field sites and in the offline mode in the laboratory to determine the spectral absorbance of waters (Avagyan et al. 2014). Thereafter, algorithms calculate solute concentrations based on absorbance at a specific wavelength or multiple wavelengths. UV-Vis sensors can be applied to detect rapid changes in response to environmental conditions. They can also be used for an adaptive sampling approach with higher sampling frequency during high-flow events such as the snowmelt period and a reduced observation frequency during the base flow period (Pellerin et al., 2012).

Recent efforts have been made to qualitatively and quantitatively characterise DOM in water bodies for ecological studies, and in-situ UV-Vis spectrophotometer plays an important role in this. Different wavelengths have been used to estimate DOC concentration from spectral absorbances.

Laudon et al., (2004) found that the absorbance at 254 nm could explain 78% to 97% of TOC concentration in seven streams. Waterloo et al. (2006) used absorbance at 255 and 350 nm as proxies for estimating DOC with calibration using a TOC analyser. Wallage and Holden (2010) tested the robustness of spectrophotometric measurements for DOC content based on absorbance at 400 nm. However, their DOC concentrations differed by up to 50% in comparison to the TOC analyser results. Therefore, methods relying on absorbance at more than one wavelength are suggested by several studies to improve the accuracy of DOC concentration measurements (Tipping et al. 2009; Sandford et al. 2010; Fichot and Benner 2011). Avagyan et al. (2014) concluded that using absorbance values as a proxy for DOC content determination should include 2-5 wavelengths in the absorbance-concentration models. Few estimates of the interference of iron concentrations by UV-Vis have been presented (Xiao et al., 2013). Iron has been suggested to contribute to the absorption of solar ultraviolet radiation either directly or through interactions with DOC. Maloney et al. (2005) found a strong correlation between total Fe and absorbance from wavelength at 320 nm.

More widespread use of UV-Vis spectrophotometers raises the question on how relationships between spectral absorbances and concentrations of various substances in water should be build and calibrated. Especially in remote sites, the acquisition of samples is expensive, and it may be difficult to obtain samples during critical high flow periods. In this article, we explore strategies for modelling DOC and Fe concentrations in three northern catchments. We compare the in-situ UV-Vis spectrophotometer to a laboratory benchtop instrument. Then we analyse the accuracy of DOC and Fe estimates from UV-Vis spectrophotometers across different rivers using multivariate methods. Especially we analyse various calibration strategies for the estimation of DOC and Fe concentrations. We compare site-specific calibration of models, to the construction of pooled models and investigate the extrapolation of DOC and Fe predictions from one catchment to another. These questions are of importance when planning the monitoring of water quality using spectral measurements in remote areas with limited calibration data.

2. Material and methods

2.1 Study site

There were three study sites in this research. Two sites locate in Krycklan, approximately 50 km northwest of the city of Umeå in northern Sweden (64˚14' N, 19 ˚46'E), where C4 (Kallkäls-myren) is a mire-dominated Svartberget sub-catchment and C5 is a lake outlet (Laudon et al., 2013; Fig. S1). The catchment area of C4 is 0.19 km^2 and 40% of it is covered by wetlands and the rest is forest. There are no lakes in the catchment. The catchment area of C5 is 0.85 km^2, of which forest accounts for 59% and wetlands constitute 36%. A small portion (5%) of the catchment is covered by a lake and the measurements were done at the lake outlet. The climate is characterised as a cold temperate humid type with persistent snow cover during the winter season. The 30-year mean annual temperature (1981–2010) is 1.8°C, January -9.5 °C, and July 14.7 °C, and the mean annual precipitation is 614 mm. During the experimental period, the average DOC and Fe concentrations were 33.01 mg L^{-1} and 1.56 mg L^{-1} in C4, 20.72 mg L^{-1} and 1.69 mg L^{-1} in C5. The pH values varied in the range of 3.94-5.75, 4.16-6.40 in C4, C5, respectively.

Yli-Nuortti measurement station (Cold station) locates in Yli-Nuortti river (67˚44' N, 29 ˚27'E) in Värriö, Finland (Fig. S1). It is about 120 km north of the Arctic Circle close to the northern timberline. The catchment covers about 40 km^2 with less than 25% of peatlands, which, however, dominating the riparian zone. Less than 5% of the area is covered by alpine vegetation while the rest of the catchment is dominated by pine forests on glacial tills. There are no lakes above the measurement station. According to the statistics of the Finnish Meteorological Institute, the mean annual air temperature is -0.5 °C. The mean temperature in January is -11.4 °C and in July 13.1 °C. The mean annual precipitation is 601mm. The average DOC and Fe concentrations were 4.96 mg L^{-1} and 0.21 mg L^{-1}, and the pH values were 6.27-6.95 during the experimental period.

2.2 Sampling and filtration

All sample bottles and reagent containers were made from high-density polyethylene and they were first cleaned in a Deko-2000 washer with detergent, then soaked for at least 24 h in 2% HNO_3, and finally rinsed six times with Milli-Q water. All glassware used in this study was additionally pre-combusted for 4 h at 450 ℃ before use.

The sampling in Yli-Nuortti river (Cold station) took place during the hydrological year 2018-2019 and in Krycklan (C4 and C5) during the hydrological years 2016-2019. In Cold station, water samples were collected monthly in winter and fall, once a fortnight in spring, and every week in summer. In Kryclan, we sampled monthly during winter, once a fortnight during summer and fall, and every third day during the spring flood. The water samples were filtered through Filtration Assembly with Whatman GF/F Glass Microfiber Filters (pore size 0.45 µm).To precondition the filtration system and avoid contamination from the filter before collecting samples, 30 ml of sample water was filtered and then discarded. The samples for absorbance measurements were preserved using $ZnCl_2$ and then stored at 4 ℃ until laboratory analysis. Samples for DOC and Fe measurements were frozen until further analysis.

2.3 Measurement of in-situ and ex-situ spectral absorbances

In site, submersible, portable multi-parameter UV–Vis probes (spectro::lyser, S::CAN Messtechnik GmbH, Austria) were used for absorbance measurements. The spectro::lyser measures absorbance across the UV–Vis range (220–732.5 nm, at 2.5 nm intervals) and saves these values in an internal datalogger. The measurement range of the probe depends on the optical path length, which can range from 2 to 100 mm. In this study, a probe with a path length of 35 mm was used. All of the control unit's electronics, including the data logger, were placed in four tubular anodised aluminium

housings. The UV–Vis probe was installed in the Yli-Nuortti river on 12 June 2018 and in the Krycklan catchments on 9 May 2016.

In the laboratory, spectral absorbance was measured with a UV-1800 UV-VIS spectrophotometer (Shimadzu, Kyoto, Japan) between 200 and 800 nm with a 10 mm pathlength quartz cell (acquisition step: 1 nm, scan speed: slow).

2.4. Measurements of DOC and Fe concentration by laboratory techniques

In Finland, dissolved organic carbon (DOC) was determined by thermal oxidation coupled with infrared detection (Multi N/C 2100, Analytik Jena, Germany) following acidification with phosphoric acid, and each sample was measured in triplicate with errors less than 3%. Fe concentrations were determined colorimetrically with ferrozine (Viollier et al., 2000) corresponding to an absorbance at 562 nm by Victor3 1420 Multilabel Counter (PerkinElmer).

In Sweden, DOC was measured with Shimadzu TOC-5000 using catalytic combustion (Laudon et al., 2004). Fe was analyzed using Inductively Coupled Plasma Optical Emission Spectroscopy (ICP-OES Varian Vista Pro Ax). To ensure the accuracy of the analysis an external certified standard (Spectrapure Standards SPS-SW1) was analyzed on a regular basis. The uncertainty was always less than 2% (Björkvald et al., 2008).

2.5. Multilinear regression methods for estimating DOC and Fe by spectral absorbance

To test for an optimised estimate of DOC and Fe from the absorbance, a set of calibrations based on three different multilinear regression methods was performed with water samples (n = 183 for DOC, n=142 for Fe). The absorbance values from 220 nm to 732.5 nm at 2.5 nm intervals (207 variables) were used as input data for Fe analyses, while wavelengths shorter than 250 nm were excluded from

the DOC analyses (194 variables) because inorganic substances can lead to interference at the lower end of the UV–Vis range (Tipping et al., 1988). The multivariate models we are using in this paper rely on splitting the data into a training and testing data set. We tried 5 different splits of the data; 1. The training set contained 75% of observations that were randomly selected from all samples (C4, C5 and Cold station) and the testing set contained the remaining 25% of observations; 2. The training set contained observations from C4 and C5 and the testing set consisted of observations from Cold station; 3. The training set contained 75% of observations randomly selected from C4 and C5 and the testing set consisted of the rest 25% of observations; 4. The training set contained 75% of observations randomly selected from C4 and Cold station and the testing set contained the rest 25% of observations; 5. The training set contained 75% of observations randomly selected from C5 and Cold station and the testing set contained the rest 25%.

The tested three statistical methods were used for the multilinear prediction of DOC and Fe concentration obtained by the laboratory measurements. Measured concentrations were always the dependent variable, and the absorbance values at different wavelengths were the independent variables. We used three methods: multiple stepwise regression (MSR), partial least-squares regression (PLS), and principal component regression (PCR). These methods were selected due to their applicability to data sets containing collinear variables and datasets that may contain a larger number of independent variables than observations. Different approaches were used for the PLS and PCR regressions. These techniques reduce the number of dimensions in the data by computing latent linear variables (Miller and Miller, 2010; Varmuza and Filzmoser, 2009). However, the method by which these linear combinations are constructed differs. In PCR, the principal components are generated to describe the maximum variation in the predictors without considering the strength of the relationship between the predictor and predictand variables (Miller and Miller, 2010). In PLS, the variables exhibiting a high correlation with the response variables are given extra weight (Miller and Miller, 2010).

The PCR and PLS analyses were conducted with '*pls'* package (Mevik et al., 2019) in R (R Core Team, 2019). Coefficients and p-values were estimated by jackknife T-test method using '*jack.test'* function in *'pls'* package. MSR analyses were performed with *'caret'* package (Wing et al., 2019) in R (R Core Team, 2019). The correlation coefficient (R), root-mean-square deviation (RMSD), standard deviation (STD) and bias were used to check the performance of the models.

3. Results

3.1 Comparison of spectral absorbance measured by two methods

Comparison of the absorbance values measured by S::CAN (average daily absorbance) and the desktop UV-1800 for the same day in 2018-2019 at Cold station reveals that the shape of absorbance curves is very similar in the wavelength range from 220 to 732.5 nm (Fig.S2). Linear regression analysis indicated that absorbances that were measured by S::CAN explained 96% of the absorbances from UV-1800, though the slope of absorbance ratios differed among days (Fig.1a). There were some exceptions from February to April when the relationships between absorbances of the two methods were not linearly correlated (Fig.1b).

Environmental factors such as water depth, temperature, turbidity and the voltage of S::CAN can be possible reasons for the differences in absorbance ratios (S::CAN / UV-1800) in different days. However, no significant linear correlations between absorbance ratio and water depth (a proxy for discharge), temperature, turbidity or the voltage of S::CAN were found (Fig.S3).

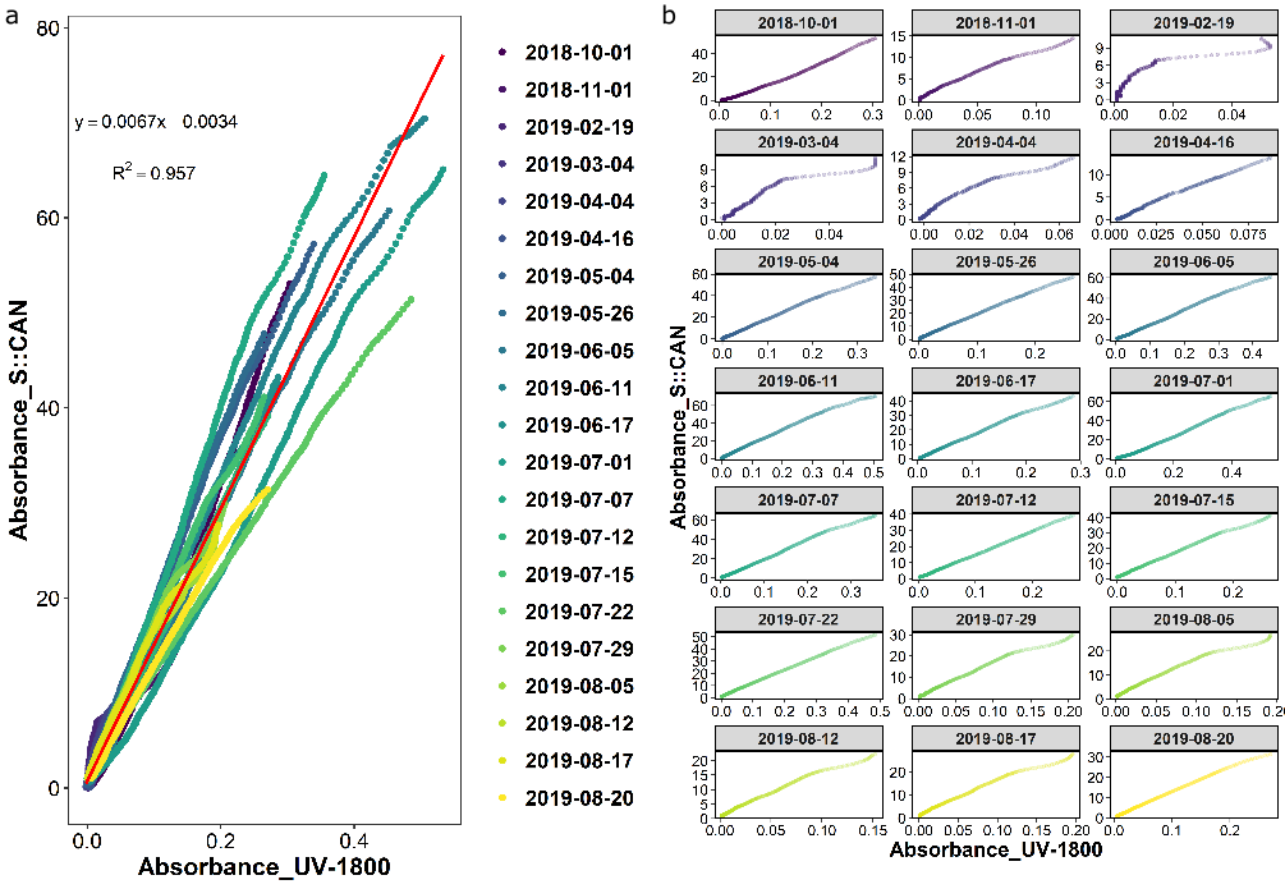

Fig.1 Relationship between Spectral absorbance measured by UV-1800 and S::CAN in different days

3.2 Comparison of multilinear models for DOC-measurement

When applied to data set 1, the DOC values from the PLS, PCR, MSR calibrations produced accurate estimates for the training set as can be seen from high explanatory power r^2 values of the models (near to 1) (Table S1), as well as for the testing set proved by the models with low root-mean-square deviations (RMSD) and high correlation coefficient values near to 1, as well as the standard deviations (STD) which are close to STD of the laboratory-measured DOC. The MSR produced the model with the highest r^2 (0.971), lowest RMSD values (2.352 mg L^{-1}) and lowest bias in each site. The PLS and PCR models performed similarly (Fig.2a).

When applied to data set 2, the DOC values from the PLS, PCR, MSR calibrations produced accurate estimates for Krycklan data set (training set) as can be seen from very low bias and high explanatory power r^2 values of the models (near to 1) (Table S2). For the testing set, the correlation coefficients and RMSD of the three models are good and very similar. STD of predicted DOC values from PLS and MSR models are close to the STD of laboratory-measured DOC values. However, the bias showed that the PLS model seemed to underestimate and PCR model over-estimate the DOC concentrations. MSR model was the best one (Fig.2b).

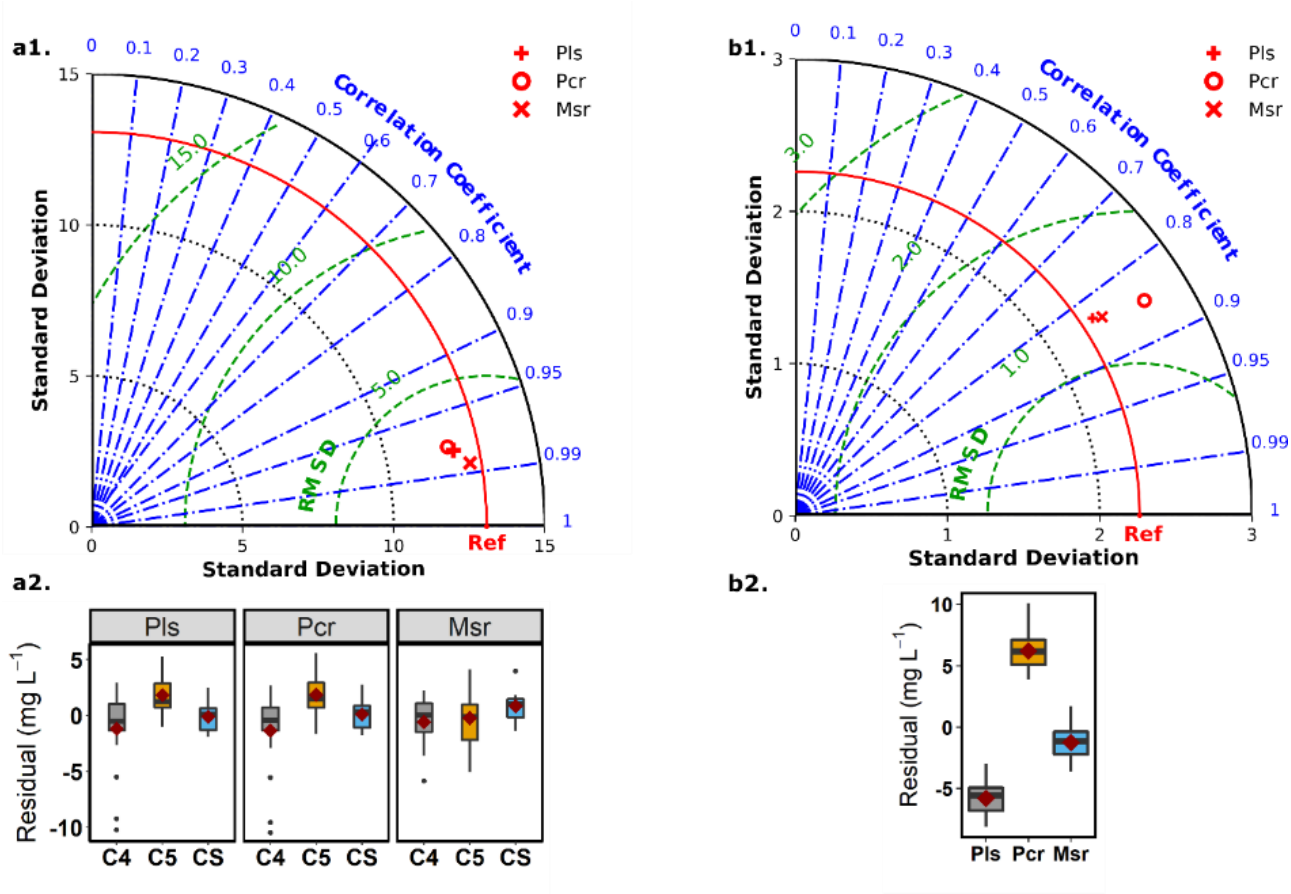

Fig.2. Statistical parameters (testing set) of partial least-squares (PLS), principal component (PCR) and multiple stepwise (MSR) regressions of estimating DOC concentration by spectral absorbance, "Ref" shows the standard deviation of the laboratory-measured DOC concentration, the diamond symbol in each box plot represents the bias. a1&2 models are based on data set 1, where the training set contains 75% of the observations (n=140) randomly selected from all samples and the testing set contains the rest 25% of the observations (n=43). b1&2 models are based on data set 2 where training and testing data are from different locations where the

training set contains the observations from C4 and C5 (n=150) and the testing set contains the observations from the Cold station (n=33).

Different combinations of spectral data from three rivers were applied to develop joint models. In each data set, the DOC values from MSR calibrations produced accurate estimates for the training set as can be seen by very high explanatory power r^2 values of the models (near to 1). For the testing set, the model performances for all data sets were good with r^2 values being higher than 0.8. The MSR calibration for data set 4 demonstrated the highest r^2, lowest RMSD values and smallest bias.

Table 1. The goodness of fit statistics of MSR regression estimating DOC by spectral absorbance for different data sets. Data set 3 is observations from C4 and C5; Data set 4 is observations from C4 and Cold station; Data set 5 is observations from C5 and Cold station. The training set contains 75% of observations that were randomly selected from each data set and the testing set contains the rest 25% of observations.

MSR	**Statistical Parameters**	**Data set 3 (C4&C5)**	**Data set 4 (C4&Cold station)**	**Data set 5 (C5&Cold station)**
Training Set	r^2	0.903	0.973	0.959
	RMSE (mg L^{-1})	3.243	2.599	1.787
Testing Set	r^2	0.942	0.976	0.802
	RMSD (mg L^{-1})	2.797	2.424	4.177
	Bias (mg L^{-1})	-0.288	-0.203	1.369

When models were built on data set 1, the normalised coefficients of PLS ($p < 0.05$) showed that the important wavelengths fell in band 250 nm to 295 nm, 310 nm to 370 nm, 377.5 nm to 410 nm, 417.5 nm to 427.5 nm and 570 nm to 580 nm while in PCR they fell in band 250 nm to 297.5 nm, 317.5 nm to 412.5 nm, 417.5 nm to 490 nm and 537.5 nm to 600 nm (Fig.3a). For data set 2, the coefficients of PLS ($p < 0.05$) showed that the important wavelengths fell in band 275 nm to 292.5 nm, 342.5 nm to 365 nm, and 570 nm to 582.5 nm, while in 250 nm to 307.5 nm, 342.5 nm to 370 nm and 412.5 nm to 440 nm in PCR (Fig.3b).

MSR method included 7 wavelengths for data set 1 (250, 290, 307.5, 437.5, 447.5, 630, 645 nm), 5 wavelengths for data set 2 (282.5, 302.5, 487.5, 645, 665 nm) and data set 3 (252.5, 255, 257.5, 447.5, 645 nm), 4 wavelengths for date set 4 (255, 260, 692.5, 722.5 nm) and data set 5 (257.5, 260, 420, 722.5 nm). In MSR models of all data sets, 645 nm was the most important wavelength, followed by 255 nm, 260 nm and 722.5 nm (Table.2).

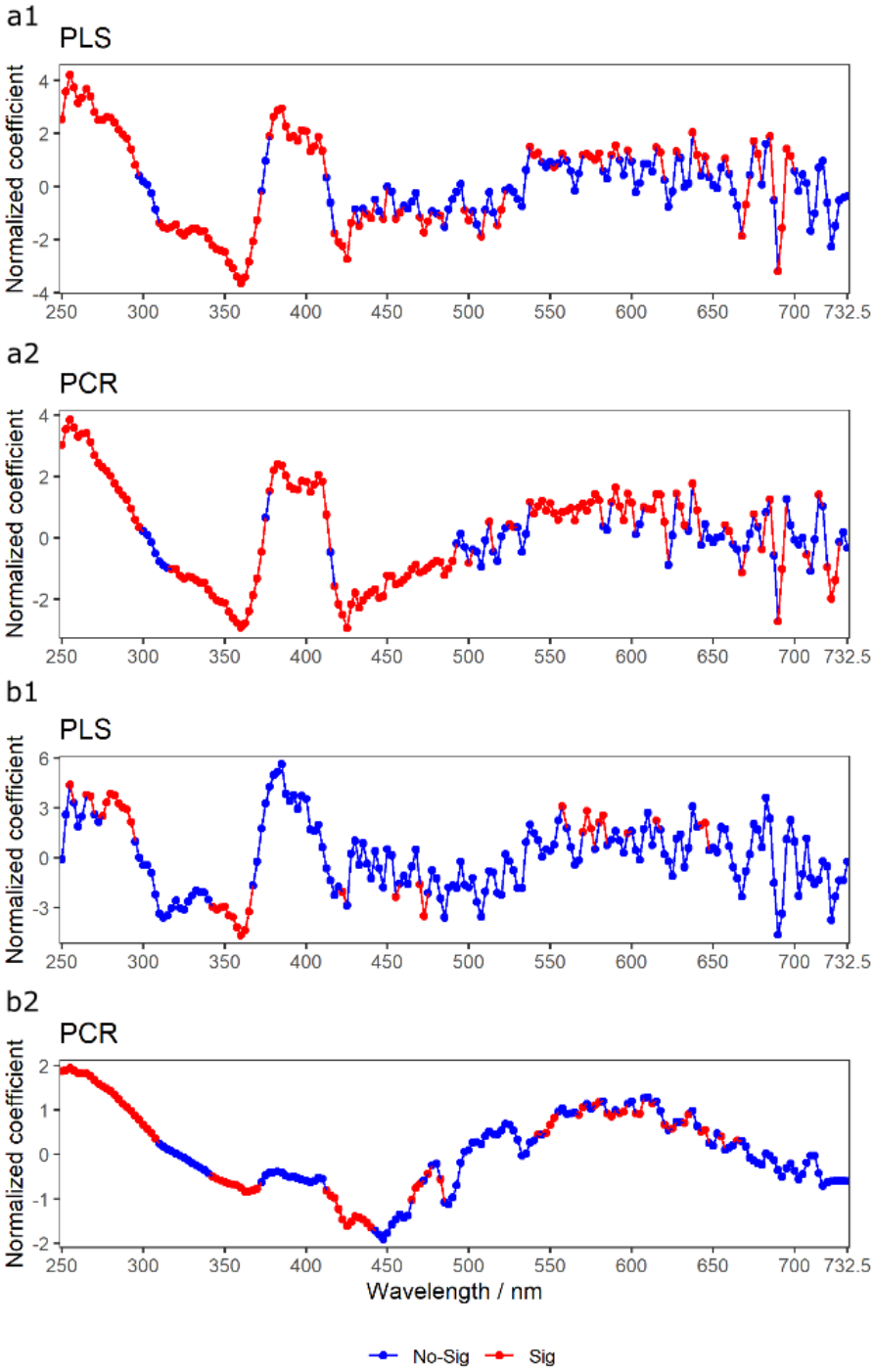

Fig.3. Normalised regression coefficients of PLS and PCR models from wavelength 250 nm to 732.5 nm at 2.5 intervals to show the effects of absorbances on DOC concentration. a1&2 models are based on data set 1 where the training set contains 75% of the observations (n=140) randomly selected from all samples, and the testing set contains the rest 25% of the observations (n=43) to check the performance of the models. b1&2 models are based on data set 2 where the training set contains observations from C4 and C5 (n=150) while the testing set contains observations from the Cold station (n=33). "Sig" indicates $p < 0.05$; "No-sig" indicates $p > 0.05$.

Table 2. Wavelengths used in MSR models for DOC and Fe prediction by different data sets.

Data sets	Number of wavelengths	Wavelengths used for DOC prediction, nm	Number of wavelengths	Wavelengths used for Fe prediction, nm
Data set 1: Training set = 75% randomly from all samples, n=140 Testing set = the rest 25%, n=43	7	250, 290, 307.5, 437.5, 447.5, 630, 645	7	227.5, 297.5, 320, 342.5, 480, 557.5, 635
Data set 2: Training set = C4&C5, n=150 Testing set = Cold station, n=33	5	305, 307.5, 632.5, 645, 692.5	-	-
Data set 3: Training set = 75% randomly from C4&C5, n=114 Testing set = the rest 25%, n=36	5	252.5, 255, 257.5, 447.5, 645	9	365, 370, 382.5, 397.5, 472.5, 480, 545, 690, 710
Data set 4: Training set = 75% randomly from C4&Cold station, n=86 Testing set = the rest 25%, n=28	4	255, 260, 692.5, 722.5	10	252.5, 262.5, 277.5, 327.5, 417.5, 455, 610, 680,707.5, 722.5
Data set 5: Training set = 75% randomly from C5& Cold station, n=72 Testing set = the rest 25%, n=24	4	257.5, 260, 420, 722.5	4	220, 222.5, 225, 230

3.3 Comparison of multilinear models for Fe -measurement

When applied to data set 1, the Fe concentrations from the PLS, PCR, MSR calibrations produced accurate estimates for the training set as can be seen from good explanatory power (r^2 values) of the models (Table S3). For the testing set, the goodness of fit was evaluated using the RMSD and the correlation coefficient. The MSR calibration method produced the model with the highest correlation coefficient, lowest RMSD, and the smallest bias in each site. (Fig.4a).

When applied to data set 2, the Fe concentrations from the PLS, PCR, and MSR calibrations produced good Fe estimates for Krycklan data set (training set) as can be seen by models with explanatory power r^2 higher than 0.45 (Table S4). However, for the Värrio testing data set the measurements applying these three calibration methods showed poor correlation coefficients and high RMSD values. (Fig.4b).

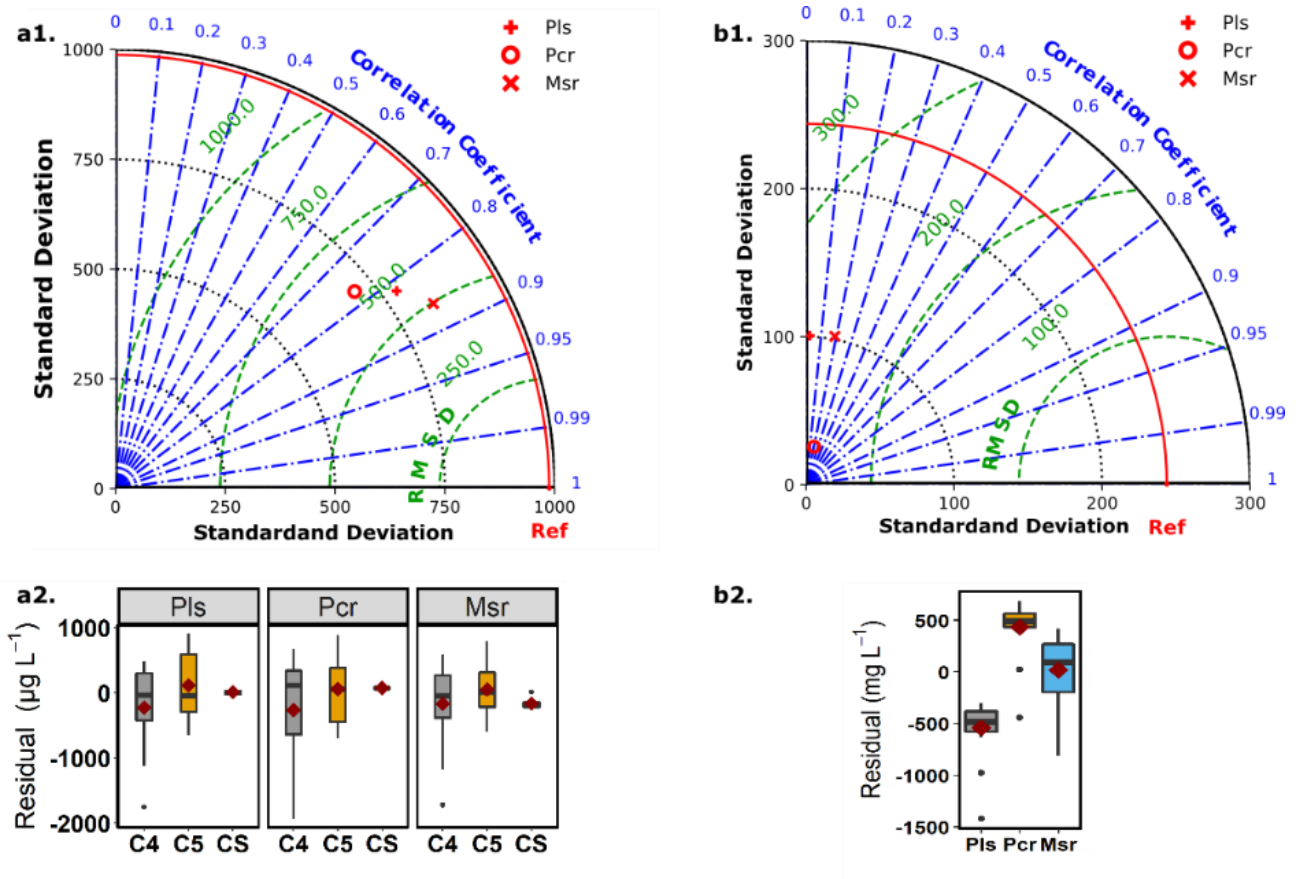

Fig.4. Statistical parameters (testing set) of partial least-squares (PLS), principal component (PCR) and multiple stepwise (MSR) models for estimating the Fe concentration by spectral absorbance. "Ref" shows the standard deviation of the laboratory-measured Fe concentrations, and the diamond symbol in each box plot represents bias (b). a1&2 models are based on data set 1 where the training set contains 75% of the observations (n=108) randomly selected from all samples and the testing set contains the rest 25% of the observations (n=34). b1&2 models are based on data set 2 where the training set contains observations from C4 and C5 (n=124), and the testing set contains observations from the Cold station (n=18).

Different combinations of spectral data from several streams were applied to develop joint models. In each data set, the predicted Fe values from the PLS calibrations produced accurate estimates for the training set as can be seen by high explanatory power r^2 values. For the testing set, the performances were not so good as with the DOC predictions. MSR calibrations by data set 4 produced the model with the highest r^2 and lowest RMSD.

Table 3. The goodness of fit statistics of the MSR regression estimating Fe by spectral absorbance for different data sets. Data set 3 is observations from C4 and C5; Data set 4 is observations from C4 and Cold station; Data set 5 is observations from C5 and Cold station. Training sets are 75% of the observations randomly selected from each data set and testing sets are the rest 25% of the observations.

MSR	Statistical Parameters	Data set 3 (C4&C5)	Data set 4 (C4&Cold station)	Data set 5 (C5&Cold station)
Training Set	r^2	0.868	0.9889	0.672
	RMSE (mg L^{-1})	287.398	108.905	473.997
Testing Set	r^2	0.583	0.876	0.623
	RMSD (mg L^{-1})	619.901	378.814	479.334
	Bias (mg L^{-1})	179.009	-124.951	78.672

For data set 1, the normalized coefficients of PLS ($p < 0.05$) showed that the important wavelengths were 225 nm, from 245 nm to 250 nm and 717.5, from 220 nm to 225 nm, from 240 nm to 282.5 nm, from 372.5 nm to 395 nm, from 440 nm to 472.5 nm, from 597.5 nm to 625 nm, from 680 nm to 685 nm and from 715 nm to 732.5 nm in PCR (Fig.5).

MSR models were based on 7 wavelengths for data set 1 (227.5, 297.5, 320, 342.5, 480, 557.5, 635 nm), 9 wavelengths for data set 3 (365, 370, 382.5, 397.5, 472.5, 480, 545, 690, 710 nm), 10 wavelengths for data set 4 (252.5, 262.5, 277.5, 327.5, 417.5, 455, 610, 680,707.5, 722.5 nm) and 4 wavelengths for data set 5 (220, 222.5, 225, 230 nm) (Table.2).

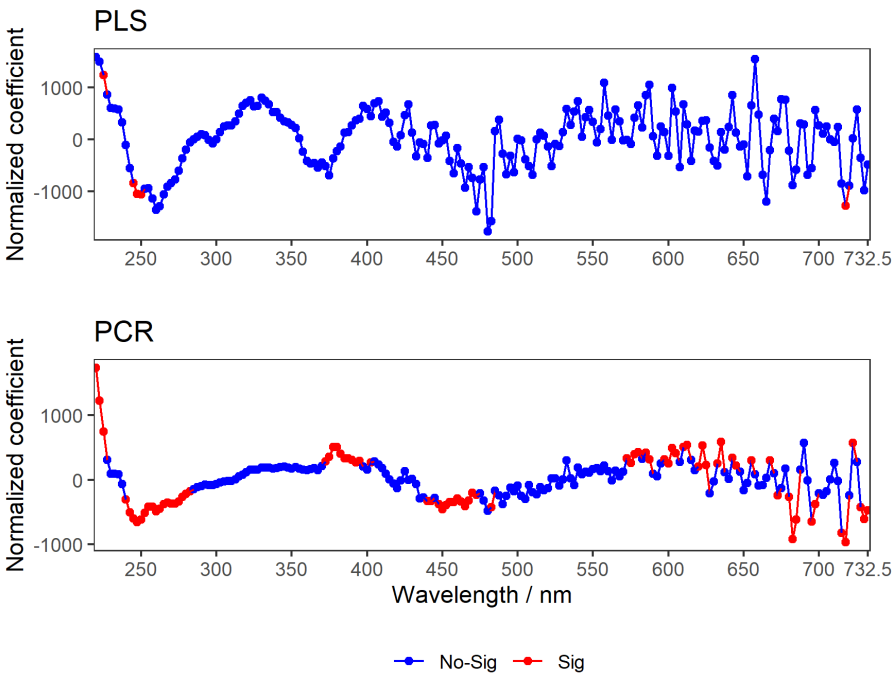

Fig.5. Normalised regression coefficients of PLS and PCR models from wavelength 220 nm to 732.5 nm at 2.5 intervals to show the effects of absorbances on iron (Fe) concentration. Models are built on data set 1, the training set contains 75% observations (n=108) randomly selected from all samples, and the testing set which was used to check the performance of the models contains the rest 25% (n=34). "Sig" indicates $p < 0.05$; "No-sig" indicates $p > 0.05$.

4. Discussion

Spectral measurement from the in-situ S: CAN uses different technologies than benchtop spectrophotometers. In situ instruments measure unfiltered water and are subject to variation in temperature. Ambient sunlight could disturb spectral measurements from the open path of the spectrophotometer and power supply is less reliable in situ than under lab conditions. A comparison of the in-situ S: CAN and the UV1800 benchtop spectrophotometer usually showed a good linear correlation between the two instruments while there was some variation in slope. We tested if differences between the ex-situ and in-situ spectra could be caused by the changes in the operating conditions. These variations in the regression slope of ex-situ on in-situ spectral absorbances were not

dependent on temperature, water level (as a proxy for water discharge) or other factors like the voltage of the power supply. This shows that in general the in-situ spectral measurements were reliable, unbiased, and not affected by water temperature, low discharge or small changes in electricity supply. There were a few occasions on non-linear correlations from February to April which can probably be explained by the ice formation on the instruments. Ice formation was caused by the compressed air used to automatically clean the instrument and not by the freezing of the river. Other possible reasons may be particles on the lenses of the instrument as well as the storage time of water samples before analysing by UV-1800. Avagyan et al. (2014) suggest that spectrophotometric measurements and laboratory method should be performed during the same day, otherwise the spectrophotometric features may change slightly during storage. In our case, the sample plot is located in remote areas which makes the sample storage unavoidable before laboratory analysis. Therefore, samples were protected using $ZnCl_2$ against microbial decomposition.

Analysis of spectral data for environmental monitoring aims to obtain reconstructions of environmental variables that are general, unbiased and accurate. We compared the performances of the three multivariate methods (PCR, PLS and MSR), and though the MSR analysis included a limited number of wavelengths in the model, it produced a model with the highest explanatory power, the lowest RMSD, and bias when applied to test data sets in different situations for both DOC and Fe predictions. Avagyan et al. (2014) found that the PCR model failed to produce accurate estimates for the testing set due to its possible over-parameterisation. In contrast, the differences in the three methods in our study were relatively minor.

Wavelengths that have previously been used as proxies for DOC concentration include 254 nm (Baker et al. 2008; Tipping et al. 2009), 272 nm (Baker et al., 2008), 320 nm (Pastor et al., 2003), 340 nm (Baker et al., 2008; Baker and Spencer, 2004; Grayson and Holden, 2012; E. Tipping et al., 2009; Tipping et al., 1988), 365 nm (Baker et al., 2008), 400 nm (Grayson and Holden, 2012; Wallage and

Holden, 2010) and 410 nm (Baker et al., 2008). Moreover, Avagyan et al. (2014) suggested that in addition to the widely used wavelength (254-400 nm), the inclusion of absorbance values at the wavelengths of 600 nm and 740 nm may significantly increase the accuracy of DOC estimates. In our case, according to PCR and PLS loadings, the most important ranges of wavelengths covered most of the widely used wavelengths in previous studies.

DOC primarily controls UV absorbance in aquatic ecosystems. The role of Fe has also been suggested to contribute to UV absorbance either directly or by interaction with DOC (Maloney et al., 2005). Moreover, Fe can also absorb UV-Vis radiation when present in mineral particles suspended in natural waters (Babin and Stramski, 2004). Wavelengths that have previously been used as proxies for Fe concentration include 245 nm (Weishaar et al., 2003), 280 nm (Weishaar et al., 2003), 320 nm (Maloney et al., 2005) and 410 (Xiao et al., 2013). In our case, according to PCR loadings, the most important ranges of wavelengths covered most of the widely used wavelengths in previous studies. In MSR models for different data sets, from 4 to 10 wavelengths were identified (Table.2).

Our study demonstrated contrasting results on the use of in situ UV-Vis spectrophotometers to estimate DOC and Fe concentrations from northern catchments. While our catchments were representative for Northern Fennoscandia, relationships between spectral absorbance and DOC (or Fe) may be different in other regions with different pH or turbidities. Spectrophotometric estimates of DOC concentrations were usually in good agreement with laboratory measurements. The spectrophotometric DOC models (PLS, PCR and MSR) explained more than 95% of the variation in DOC in our data when we used DOC measurements from three catchments for the calibration of the relationship. Additionally, our analysis suggests that it is possible to develop joint models by combining spectral and calibration data from several rivers, reducing the need to acquire physical water samples for calibration of new sensor applications. The joint calibration of all three sites resulted in low bias and a high R^2. Even the spectrophotometric DOC model based only on observations from

Krycklan, Sweden did fit to measurements from Lapland, Finland reasonably well. The standard deviation of the predicted data was similar to the standard deviation of measured data indicating that the analysis was able to capture extreme events and that it had a realistic variance of measured values.

In contrast, the spectrophotometric estimates of Fe concentrations were not as good as DOC measurements. The spectrophotometric Fe models (PLS, PCR and MSR) explain about 65% of the variation in Fe concentrations. However, spectrophotometric Fe models based on data from Krycklan, Sweden did not fit to measurements from the catchment in Lapland, Finland. Gledhill et al. (2004) found that in waters with pH >5, the concentration of inorganic free ferric Fe is very low, and the dissolved Fe is primarily associated with dissolved organic ligands such as humic substances and siderphores. In our case, pH in the Cold station (6.27-6.95) was much higher than in C4 (3.94-5.75) and in C5 (4.16-6.4). Additionally, the difference of soil redox conditions from one site to another could affect the results as well. In our study, the Krycklan catchments are more peatland dominated than the catchment in Finland. In peatland environments redox processes are predominant and they are the main source of terrestrial Fe in surface waters. The effect of Fe on watercolour varies depending on its oxidation state, hydration, and chemical complexation (Sarkkola et al., 2013). Furthermore, the reason why Krycklan spectrophotometric Fe models do not fit to the estimates from Finnish Lapland could also be explained by the huge difference in Fe concentrations. In C4 and C5 of Krycklan, the concentration were 155 to 3730 µg L^{-1}, and in Cold station of Lapland 32 to 539 µg L^{-1}.

The results indicate that our model was successful for building accurate and unbiased models for multiple watersheds for DOC. The models were, at a certain loss of precision, appropriate to be extrapolated from one watershed to another even without site-specific calibration for DOC. However, for Fe the combination of different datasets was not possible. This means that the remote DOC sensors based on spectrophotometry could operate with a low number of samples and that a set of DOC sensors could be calibrated jointly with little loss of accuracy, but the same approach seems to be not working well for Fe.

5. Conclusions

The in-situ S: CAN worked well except for February to April when the ice formation on the instruments may have somehow reduced the accuracy. Eventhough, this did not affect successfully using absorbance from S: CAN to build accurate and unbiased models for multiple watersheds for DOC, and these models could be extrapolated from one watershed to another even without site-specific calibration for DOC. For Fe the combination of different datasets was not possible. This means that the remote DOC sensors based on spectrophotometry could be calibrated with a low number of samples but the same approach is not working well for Fe. Comparison of the performance of the three multivariate methods (PCR, PLS and MSR) indicated that MSR lead to the best model for both DOC and Fe predictions. Same research in different regions around the world should be conducted in the future to prove the versatility of our proposed models.

Acknowledgement

This work was supported through Kone project (201906598) - 'The role of terrestrial productivity on fluxes of dissolved organic carbon in watersheds (Maaekosysteemien tuottavuuden merkitys liukoisen orgaanisen hiilen virtoihin valuma-alueilla)' and the Water JPI and Academy of Finland project REFORMWATER (Academy of Finland project number 326818). The Krycklan Catchment Study is funded by the Swedish Infrastructure for Ecosystem Science (SITES), the VR extreme event project, the Swedish Research Council for Sustainable Development (FORMAS) and SKB, while the high frequency work is supported by the European Union's Horizon 2020 Research and Innovation Programme under the Marie Sklodowska - Curie Grant Agreement No 734317.

Reference

Asmala, E., Carstensen, J., Räike, A., 2019. Multiple anthropogenic drivers behind upward trends in organic carbon concentrations in boreal rivers. Environ. Res. Lett. 14, 124018. https://doi.org/10.1088/1748-9326/ab4fa9

Aufdenkampe, A.K., Mayorga, E., Raymond, P.A., Melack, J.M., Doney, S.C., Alin, S.R., Aalto, R.E., Yoo, K., 2011. Riverine coupling of biogeochemical cycles between land, oceans, and atmosphere. Front. Ecol. Environ. 9, 53–60. https://doi.org/10.1890/100014

Avagyan, A., Runkle, B.R.K., Kutzbach, L., 2014. Application of high-resolution spectral absorbance measurements to determine dissolved organic carbon concentration in remote areas. J. Hydrol. 517, 435–446. https://doi.org/10.1016/j.jhydrol.2014.05.060

Babin, M., Stramski, D., 2004. Variations in the mass-specific absorption coefficient of mineral particles suspended in water. Limnol. Oceanogr. 49, 756–767. https://doi.org/10.4319/lo.2004.49.3.0756

Baker, A., Bolton, L., Newson, M., Spencer, R.G.M., 2008. Spectrophotometric properties of surface water dissolved organic matter in an afforested upland peat catchment. Hydrol. Process. 22, 2325–2336. https://doi.org/10.1002/hyp.6827

Baker, A., Spencer, R.G.M., 2004. Characterization of dissolved organic matter from source to sea using fluorescence and absorbance spectroscopy. Sci. Total Environ. 333, 217–232. https://doi.org/10.1016/j.scitotenv.2004.04.013

Björkvald, L., Buffam, I., Laudon, H., Mörth, C.-M., 2008. Hydrogeochemistry of Fe and Mn in small boreal streams: The role of seasonality, landscape type and scale. Geochim. Cosmochim. Acta 72, 2789–2804. https://doi.org/10.1016/j.gca.2008.03.024

Chittoor Viswanathan, V., Molson, J., Schirmer, M., 2015. Does river restoration affect diurnal and seasonal changes to surface water quality? A study along the Thur River, Switzerland. Sci. Total Environ. 532, 91–102. https://doi.org/10.1016/j.scitotenv.2015.05.121

Cole, J.J., Prairie, Y.T., Caraco, N.F., McDowell, W.H., Tranvik, L.J., Striegl, R.G., Duarte, C.M., Kortelainen, P., Downing, J.A., Middelburg, J.J., Melack, J., 2007. Plumbing the Global Carbon Cycle: Integrating Inland Waters into the Terrestrial Carbon Budget. Ecosystems 10, 172–185. https://doi.org/10.1007/s10021-006-9013-8

Erlandsson, M., Buffam, I., Fölster, J., Laudon, H., Temnerud, J., Weyhenmeyer, G.A., Bishop, K., 2008. Thirty-five years of synchrony in the organic matter concentrations of Swedish rivers explained by variation in flow and sulphate. Glob. Change Biol. 14, 1191–1198. https://doi.org/10.1111/j.1365-2486.2008.01551.x

Erlandsson, M., Cory, N., Fölster, J., Köhler, S., Laudon, H., Weyhenmeyer, G.A., Bishop, K., 2011. Increasing Dissolved Organic Carbon Redefines the Extent of Surface Water Acidification and Helps Resolve a Classic Controversy. BioScience 61, 614–618. https://doi.org/10.1525/bio.2011.61.8.7

Fichot, C.G., Benner, R., 2011. A novel method to estimate DOC concentrations from CDOM absorption coefficients in coastal waters: DOC ESTIMATES FROM CDOM ABSORPTION COEFFICIENTS. Geophys. Res. Lett. 38, n/a-n/a. https://doi.org/10.1029/2010GL046152

Gledhill, M., McCormack, P., Ussher, S., Achterberg, E.P., Mantoura, R.F.C., Worsfold, P.J., 2004. Production of siderophore type chelates by mixed bacterioplankton populations in nutrient enriched seawater incubations. Mar. Chem. 88, 75–83. https://doi.org/10.1016/j.marchem.2004.03.003

Grayson, R., Holden, J., 2012. Continuous measurement of spectrophotometric absorbance in peatland streamwater in northern England: implications for understanding fluvial carbon fluxes. Hydrol. Process. 26, 27–39. https://doi.org/10.1002/hyp.8106

Haaland, S., Hongve, D., Laudon, H., Riise, G., Vogt, R.D., 2010. Quantifying the Drivers of the Increasing Colored Organic Matter in Boreal Surface Waters. Environ. Sci. Technol. 44, 2975–2980. https://doi.org/10.1021/es903179j

Hongve, D., Riise, G., Kristiansen, J.F., 2004. Increased colour and organic acid concentrations in Norwegian forest lakes and drinking water – a result of increased precipitation? Aquat. Sci. 66, 231–238. https://doi.org/10.1007/s00027-004-0708-7

Jacobs, S.R., Weeser, B., Rufino, M.C., Breuer, L., 2020. Diurnal Patterns in Solute Concentrations Measured with In Situ UV-Vis Sensors: Natural Fluctuations or Artefacts? Sensors 20, 859. https://doi.org/10.3390/s20030859

Kirchner, J.W., Feng, X., Neal, C., Robson, A.J., 2004. The fine structure of water-quality dynamics: the (high-frequency) wave of the future. Hydrol. Process. 18, 1353–1359. https://doi.org/10.1002/hyp.5537

Krause, S., Lewandowski, J., Dahm, C.N., Tockner, K., 2015. Frontiers in real-time ecohydrology – a paradigm shift in understanding complex environmental systems. Ecohydrology 8, 529–537. https://doi.org/10.1002/eco.1646

Langergraber, G., Fleischmann, N., Hofstädter, F., 2003. A multivariate calibration procedure for UV/VIS spectrometric quantification of organic matter and nitrate in wastewater. Water Sci. Technol. 47, 63–71.

Laudon, H., Köhler, S., Buffam, I., 2004. Seasonal TOC export from seven boreal catchments in northern Sweden. Aquat. Sci. - Res. Boundaries 66, 223–230. https://doi.org/10.1007/s00027-004-0700-2

Laudon, H., Taberman, I., Ågren, A., Futter, M., Ottosson-Löfvenius, M., Bishop, K., 2013. The Krycklan Catchment Study—A flagship infrastructure for hydrology, biogeochemistry, and climate research in the boreal landscape. Water Resour. Res. 49, 7154–7158. https://doi.org/10.1002/wrcr.20520

Maloney, K.O., Morris, D.P., Moses, C.O., Osburn, C.L., 2005. The Role of Iron and Dissolved Organic Carbon in the Absorption of Ultraviolet Radiation in Humic Lake Water. Biogeochemistry 75, 393–407. https://doi.org/10.1007/s10533-005-1675-3

McDowell, W.H., 2015. NEON and STREON: opportunities and challenges for the aquatic sciences. Freshw. Sci. 34, 386–391. https://doi.org/10.1086/679489

Mercado, L.M., Bellouin, N., Sitch, S., Boucher, O., Huntingford, C., Wild, M., Cox, P.M., 2009. Impact of changes in diffuse radiation on the global land carbon sink. Nature 458, 1014–1017. https://doi.org/10.1038/nature07949

Mevik, B.-H., Wehrens, R., Liland, K.H., 2019. pls: Partial Least Squares and Principal Component Regression.

Miller, J.N., Miller, J.C., 2010. Statistics and Chemometrics for Analytical Chemistry, 6th Edition.

Pastor, J., Solin, J., Bridgham, S.D., Updegraff, K., Harth, C., Weishampel, P., Dewey, B., 2003. Global warming and the export of dissolved organic carbon from boreal peatlands. Oikos 100, 380–386. https://doi.org/10.1034/j.1600-0706.2003.11774.x

Pellerin, B.A., Saraceno, J.F., Shanley, J.B., Sebestyen, S.D., Aiken, G.R., Wollheim, W.M., Bergamaschi, B.A., 2012. Taking the pulse of snowmelt: in situ sensors reveal seasonal, event and diurnal patterns of nitrate and dissolved organic matter variability in an upland forest stream. Biogeochemistry 108, 183–198. https://doi.org/10.1007/s10533-011-9589-8

Peltomaa, E., Ojala, A., Holopainen, A.-L., Salonen, K., 2014. Changes in phytoplankton in a boreal lake during a 14-year period 18, 14.

R Core Team, 2019. R: A Language and Environment for Statistical Computing. R Foundation for Statistical Computing, Vienna, Austria.

Raymond, P.A., Saiers, J.E., Sobczak, W.V., 2016. Hydrological and biogeochemical controls on watershed dissolved organic matter transport: pulse-shunt concept. Ecology 97, 5–16. https://doi.org/10.1890/14-1684.1

Rode, M., Wade, A.J., Cohen, M.J., Hensley, R.T., Bowes, M.J., Kirchner, J.W., Arhonditsis, G.B., Jordan, P., Kronvang, B., Halliday, S.J., Skeffington, R.A., Rozemeijer, J.C., Aubert, A.H.,

Rinke, K., Jomaa, S., 2016a. Sensors in the Stream: The High-Frequency Wave of the Present. Environ. Sci. Technol. 50, 10297–10307. https://doi.org/10.1021/acs.est.6b02155

Rode, M., Wade, A.J., Cohen, M.J., Hensley, R.T., Bowes, M.J., Kirchner, J.W., Arhonditsis, G.B., Jordan, P., Kronvang, B., Halliday, S.J., Skeffington, R.A., Rozemeijer, J.C., Aubert, A.H., Rinke, K., Jomaa, S., 2016b. Sensors in the Stream: The High-Frequency Wave of the Present. Environ. Sci. Technol. 50, 10297–10307. https://doi.org/10.1021/acs.est.6b02155

Sandford, R.C., Bol, R., Worsfold, P.J., 2010. In situ determination of dissolved organic carbon in freshwaters using a reagentless UV sensor. J. Environ. Monit. 12, 1678. https://doi.org/10.1039/c0em00060d

Sarkkola, S., Nieminen, M., Koivusalo, H., Laurén, A., Kortelainen, P., Mattsson, T., Palviainen, M., Piirainen, S., Starr, M., Finér, L., 2013. Iron concentrations are increasing in surface waters from forested headwater catchments in eastern Finland. Sci. Total Environ. 463–464, 683–689. https://doi.org/10.1016/j.scitotenv.2013.06.072

Tipping, Edward, Corbishley, H.T., Koprivnjak, J.-F., Lapworth, D.J., Miller, M.P., Vincent, C.D., Hamilton-Taylor, J., 2009. Quantification of natural DOM from UV absorption at two wavelengths. Environ. Chem. 6, 472–476. https://doi.org/10.1071/EN09090

Tipping, E., Corbishley, H.T., Koprivnjak, J.-F., Lapworth, D.J., Miller, M.P., Vincent, C.D., Hamilton-Taylor, J., 2009. Quantification of natural DOM from UV absorption at two wavelengths. Environ. Chem. 6, 472–476. https://doi.org/10.1071/EN09090

Tipping, E., Hilton, J., James, B., 1988. Dissolved organic matter in Cumbrian lakes and streams. Freshw. Biol. 19, 371–378. https://doi.org/10.1111/j.1365-2427.1988.tb00358.x

Varmuza, K., Filzmoser, P., 2009. Principal component analysis. Introd. Multivar. Stat. Anal. Chemom. 1–0.

Viollier, E., Inglett, P.W., Hunter, K., Roychoudhury, A.N., Van Cappellen, P., 2000. The ferrozine method revisited: Fe(II)/Fe(III) determination in natural waters. Appl. Geochem. 15, 785–790. https://doi.org/10.1016/S0883-2927(99)00097-9

Wallage, Z.E., Holden, J., 2010. Spatial and temporal variability in the relationship between water colour and dissolved organic carbon in blanket peat pore waters. Sci. Total Environ. 408, 6235–6242. https://doi.org/10.1016/j.scitotenv.2010.09.009

Waterloo, M.J., Oliveira, S.M., Drucker, D.P., Nobre, A.D., Cuartas, L.A., Hodnett, M.G., Langedijk, I., Jans, W.W.P., Tomasella, J., Araújo, A.C. de, Pimentel, T.P., Estrada, J.C.M., 2006. Export of organic carbon in run-off from an Amazonian rainforest blackwater catchment. Hydrol. Process. 20, 2581–2597. https://doi.org/10.1002/hyp.6217

Weishaar, J.L., Aiken, G.R., Bergamaschi, B.A., Fram, M.S., Fujii, R., Mopper, K., 2003. Evaluation of Specific Ultraviolet Absorbance as an Indicator of the Chemical Composition and Reactivity of Dissolved Organic Carbon. Environ. Sci. Technol. 37, 4702–4708. https://doi.org/10.1021/es030360x

Wing, M.K.C. from J., Weston, S., Williams, A., Keefer, C., Engelhardt, A., Cooper, T., Mayer, Z., Kenkel, B., Team, the R.C., Benesty, M., Lescarbeau, R., Ziem, A., Scrucca, L., Tang, Y., Candan, C., Hunt, T., 2019. caret: Classification and Regression Training.

Xiao, Y.-H., Sara-Aho, T., Hartikainen, H., Vähätalo, A.V., 2013. Contribution of ferric iron to light absorption by chromophoric dissolved organic matter. Limnol. Oceanogr. 58, 653–662. https://doi.org/10.4319/lo.2013.58.2.0653